IEEE Power Electronics Magazine, vol. 7, no. 2, pp. 53–63, 2020

On Power Scalability of Modular Multilevel Converters: Increasing Current Ratings Through Branch Paralleling

S. Milovanovic and D. Dujic

POWER ELECTRONICS LABORATORY
ÉCOLE POLYTECHNIQUE FÉDÉRALE DE LAUSANNE

by Stefan Milovanovic and Drazen Dujic

On Power Scalability of Modular Multilevel Converters

Increasing current ratings through branch paralleling

The modular multilevel converter (MMC) presented in Figure 1 found its place within high-voltage and medium-voltage (MV) applications owing to the possibility of effortlessly meeting the imposed voltage requirements by stacking the so-called submodules (SMs) in a series [1]. Therefore, high-quality voltage waveforms can be synthesized across the MMC ac terminals, while using the power devices of a lower voltage rating, resulting in a very modest or even no filtering requirement on the grid side. Depending on the application, the SMs are mainly half bridge (HB) or full bridge (FB), not including the other types of SMs reported in the literature [2]. According to Figure 1, a cluster of SMs in a series connection with an inductor L_{br} will be referred to as the *branch*, whereas two branches comprise the *leg*.

With power being the product of voltage and current, it might seem that unlimited power ratings can be achieved by increasing the rated voltage of an MMC through the installation of a higher number of SMs into its branches. However, such a claim is only partially correct. Namely, the applications in which the voltage can be freely selected exist and, in these cases, high power ratings (e.g., 500 MW) are indeed achieved by relying on the aforementioned principle. Typical examples refer to the high-voltage power transmission, in which several hundred megawatts are transferred across the power lines operating at several hundreds of kilovolts. On the other hand, the use of an MMC has also been investigated in the applications, such as the MV drives [3], where the operating voltages are well defined (e.g., 3.3-, 6-, and 11-kV drives). With the standardized application voltages, an increase in the MMC power

Digital Object Identifier 10.1109/MPEL.2020.2984350
Date of current version: 16 June 2020

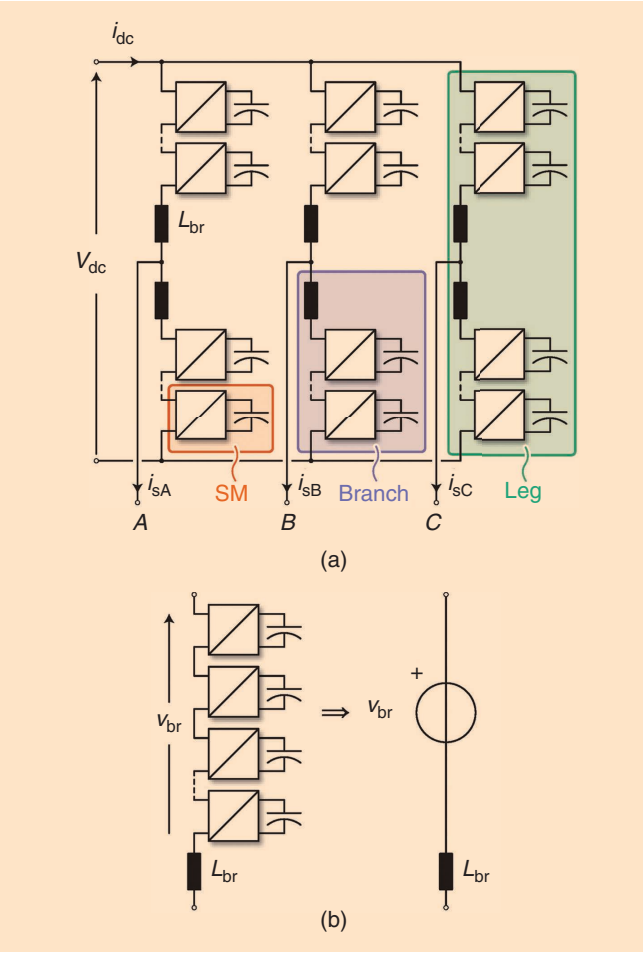

FIG 1 (a) An MMC. (b) As every branch provides the possibility for high-quality voltage generation, it can be modeled with an ideal voltage source.

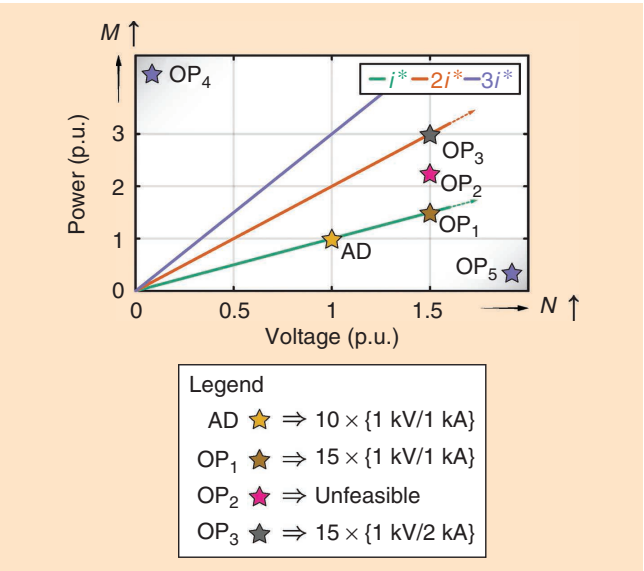

FIG 2 The MMC power scalability depending on the available SM design. The availability of an SM with rated voltage and current equal to 1 kV and 1 kA was assumed, whereas the normalization basis for the operating voltage of an observed converter was adopted as 10 kV. As the OP_2 cannot be reached unless additional modifications of the SMs are performed, it was characterized as the unfeasible operating point (concerning the existing SM design).

rating implies its current capacity boost, which may not always be trivial to accomplish.

Let one observe an exemplary case with the MMC being connected to a 10-kV dc network while employing the SMs designed to withstand the voltage and current equal to 1 kV and 1 kA, respectively. This SM design will be referred to as the *available design* (*AD*), while 10 kV represents the normalization basis regarding the converter dc voltage.

In the analyzed case and using simplified calculation, the number of SMs per branch can be determined as $N = 10\text{ kV}/1\text{ kV} = 10$. In the power-voltage (P-V) diagram from Figure 2, such an operating point was labeled with the yellow star [$v^* = 1$ per unit (p.u.) and $p^* = 1$ p.u.]. If, for example, five SMs are added into every branch of the analyzed MMC, the voltage it can interface at its dc terminals increases to 15 kV ($v^* = 1.5$ p.u.). As the SM current rating is unchanged, the rated power of the converter gets scaled linearly. In other words, changing the number of series-connected SMs within a branch causes the converter operating point (OP) to slide along the green line in Figure 2. Hence, the point OP_1 indicates an increased number of series-connected SMs ($N = 15$) with respect to the converter operating at voltage equal to 1 p.u. ($N = 10$), yet with the same current rating.

However, to meet the requirements of any application with an OP residing above the green line, the current handling capabilities of the converter must be increased. If an application operates at the OP_2 (15 kV, 1.5 kA), reusing the available SMs is not possible owing to the current rating insufficiency, even if the application's voltage requirements are met. A new SM could be designed to meet the application needs; however, this comes with an additional research and development cost. Providing that a new SM with twice the initial current rating is available, the newly designed system ratings allow OP_3 to be reached. However, the system operating voltage remains unchanged, as indicated in Figure 2.

While the OP_2 can be served now, the actual MMC has significantly higher ratings than required and is likely to be more expensive than needed. A further increase of the SM current rating (e.g., three times the initial current) gives another capability line in the P-V plane and provides insight into the MMC scalability. It is noteworthy that reaching the power-scaling plot corner points (e.g., OP_4: high power–low voltage or OP_5: low power–high voltage) would likely not be reasonable economy-wise or practical in engineering terms. In other words, despite many advantages, the MMC has its own limitations regarding the span of OPs that can be served with satisfactory economic and technical efficiency. Moreover, the current, and simultaneously the power, capacity boost is rather a nontrivial task with several technical challenges as described next.

MMC Scalability Options

The parallel connection of power modules (PMs), as shown in Figure 3(a), is widely used for monolithic converters such

as the neutral point clamped, flying capacitor, cascaded H-bridge converter, and so on. It can also be used for the MMC, providing that considerations on different static and dynamic characteristics of the employed modules [4], [5] are considered. However, if a single SM design is to serve an application with several current ratings (e.g., 100 A, 200 A, and 300 A), the cooling system, as well as the overall form factor, are likely determined for the highest of considered currents. More importantly, paralleling of the PMs implies a higher SM capacitance, and implicitly the volumetric requirements, since the SM energy oscillations increase proportionally to its current rating [6].

Despite many advantages, the MMC has its own limitations regarding the span of OPs that can be served with satisfactory economic and technical efficiency.

Figure 3(b) illustrates the extension of the MMC current capacity through the paralleling of HB (or FB) SMs [7]. There are few downsides to this approach: 1) positive terminals of the SM capacitors should also be connected, with the aim of equalizing the voltage across all of the SMs and, as a result, an additional terminal(s) must be provided; 2) small, nevertheless, additional inductances L_σ must be installed in a series with every SM considering its voltage source nature; and 3) since paralleled SMs are normally switched on/off simultaneously, the synchronization among the gate signals, or specially designed driver master/slave structure, must also be provided. Figure 3(c) presents an obvious choice of an arbitrary number of converters operating in parallel, which is a well-known and widely used power-increase method; hence, it is not discussed further in this article.

The previously presented MMC power-extension options can be considered to be state of the art. Interestingly, the existing literature does not consider another power-extension option, which alleviates many of the mentioned problems while providing certain advantages. Namely, the MMC current capacity increase can also be achieved through the paralleling of the branches [8], as presented in Figure 3(d). Since the branch represents the topological feature specific to the MMC, the identical approach can be employed in all MMC-alike circuits (e.g., matrix MMC, Δ-STATCOM, and so on).

In this case, the existing SMs can be reused without the need to undergo any major redesign process and power scaling of the MMC gets substantially facilitated, yet with the constraints are imposed solely by the employed control platform. To retain the naming consistency, what has been referred to as the branch so far, will henceforth be referred to as the *subbranch* (*SBR*). However, the following two challenges must be addressed:

- equal current sharing among the SBRs
- equal energy distribution among the SBRs.

Modeling and Control of the MMC Operating With Parallel SBRs

Figure 4 presents the MMC operating in this configuration. The number of series-connected SMs within an SBR is denoted by N, whereas M denotes the number of parallel SBRs within a branch.

Adopting the modeling approach illustrated in Figure 1(b) provides the framework for the modeling of a branch of the MMC depicted in Figure 4(a)–(c). As illustrated in Figure 5(a) and (b), a set of parallel SBRs can be replaced with an equivalent voltage source, in a series connection with an equivalent impedance. As a result, the equivalent circuit of an MMC operating with parallel branches does not differ from the equivalent circuit of a conventional MMC, as indicated in Figure 5(c). Consequently, identical principles of the terminal currents control [9] are retained.

Given that simultaneous control of both dc and ac terminal currents needs to be established, every branch produces the voltage consisting of two components, as illustrated in Figure 6. Voltage components labeled with $\overline{v_{c\{A/B/C\}\Sigma}}$ contribute to the control of the MMC dc current i_{dc}. On the other hand, voltage components $\overline{v_{s\{A/B/C\}\Sigma}}$ control the MMC ac currents $i_{s\{A/B/C\}}$. Both $\overline{v_{c\{A/B/C\}}}$ and $\overline{v_{s\{A/B/C\}}}$ are provided by the so-called higher control layers.

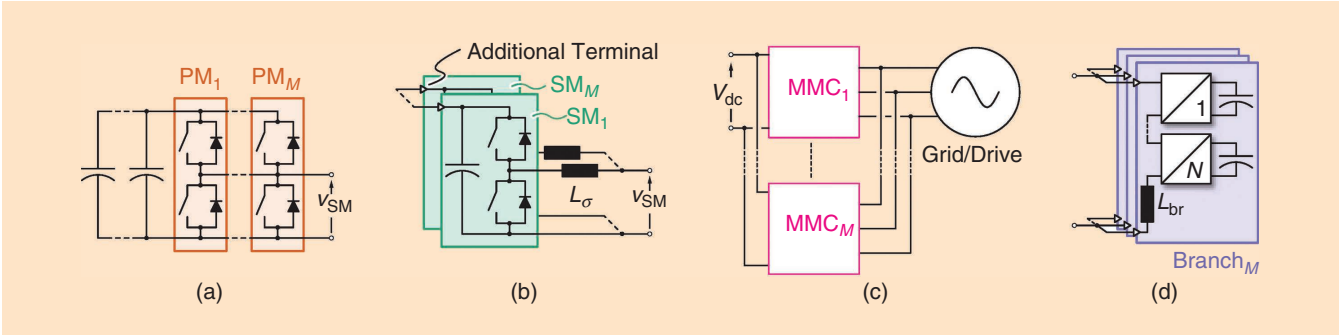

FIG 3 The parallel connection of (a) PMs within an SM, (b) SMs, (c) an arbitrary number of MMCs, and (d) the MMC branches.

To control the terminal currents, the higher control layers provide each of the branches with voltage reference labeled with v_{br}^{*}. Nevertheless, the reference v_{br}^{*} is generated through the joint action of M parallel connected SBRs, as presented in Figure 5. Hence, there are M degrees of freedom regarding the realization of the component v_{br}^{*}.

At first instance, let one assume that $v_{\mathrm{br},i} = v_{\mathrm{br}}^{*}$ holds. Since a practical realization of the SBR impedances without any deviations from the rated parameters (for instance, $\Delta Z_{\mathrm{br}} = \pm 20\%$) cannot be avoided, passing the identical voltage reference to all of the SBRs causes the unequal current, and consequently power, sharing among them.

Therefore, to establish the equal SBR current sharing, an SBR voltage should be realized as $v_{\mathrm{br},i} = v_{\mathrm{br}}^{*} + \Delta v_{\mathrm{br},i}$, where $\Delta v_{\mathrm{br},i}$ denotes an individual SBR voltage deviation from the reference provided by the higher control layers. However, establishing the equal SBR current sharing does not lead to the equal energy distribution among the SBRs. On the contrary, since $v_{\mathrm{br},1} \neq v_{\mathrm{br},2} \neq \cdots \neq v_{\mathrm{br},M}$, while $i_{\mathrm{br},1} = i_{\mathrm{br},2} = \cdots = i_{\mathrm{br},M}$ holds, the SBR powers differ from each other, causing the divergence in the SBR energies. From here, one can conclude that balancing the SBR currents opposes the balancing of the SBR energies, which can be graphically presented as in Figure 7.

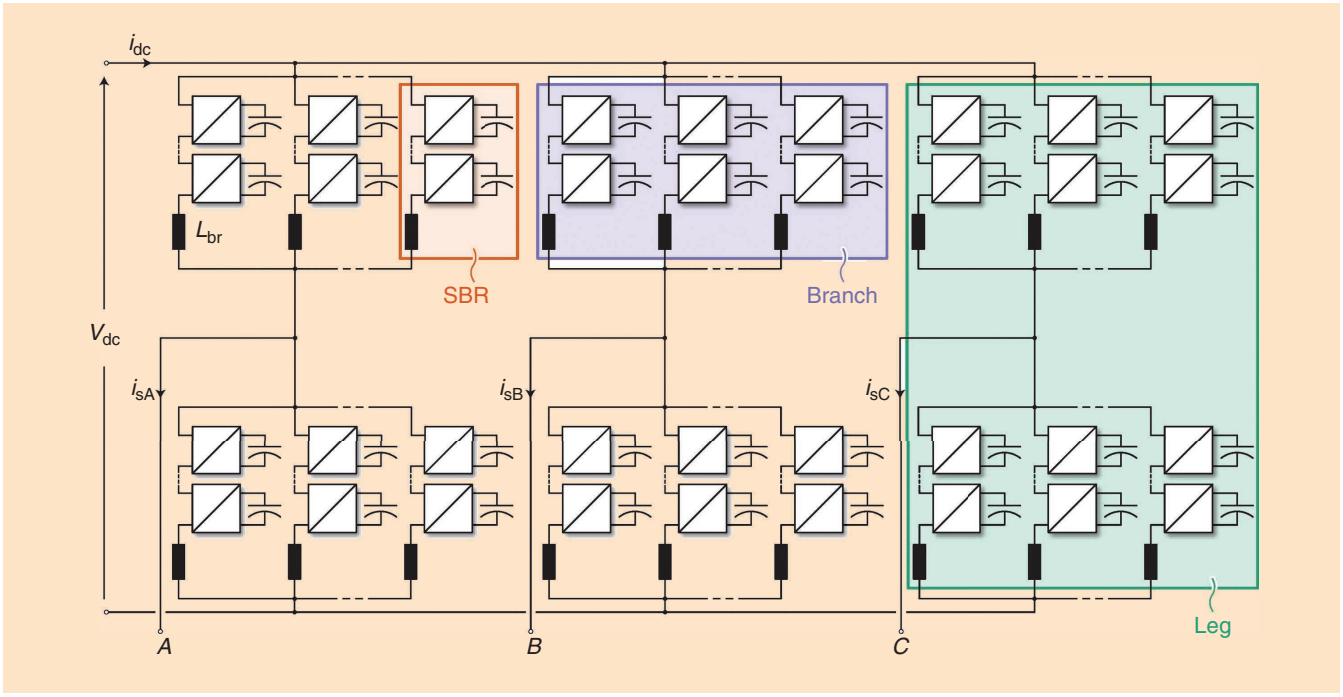

FIG 4 The MMC operating with parallel SBRs.

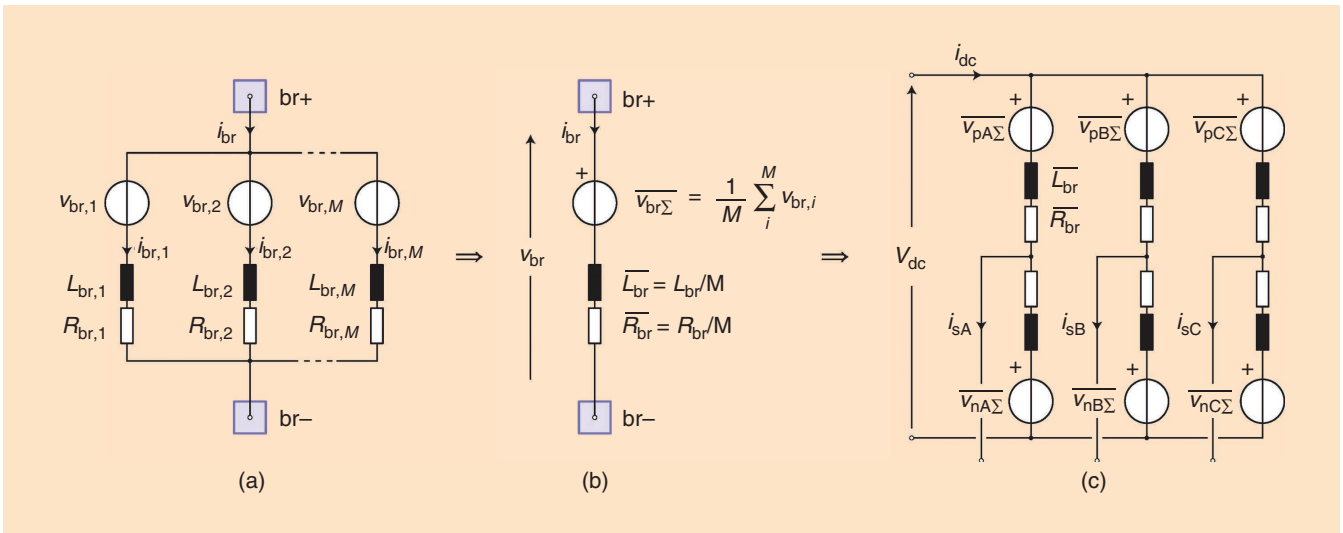

FIG 5 Since every SBR generates a high-quality voltage, the modeling approach presented in Figure 1(b) can be relied upon. According to Thevenin's theorem, (a) a set of parallel SBRs can be represented by (b) the equivalent consisting of a voltage source in series connection with an equivalent impedance. (c) Consequently, the model of an MMC operating with parallel SBRs does not differ from the conventional MMC illustrated in Figure 1(a).

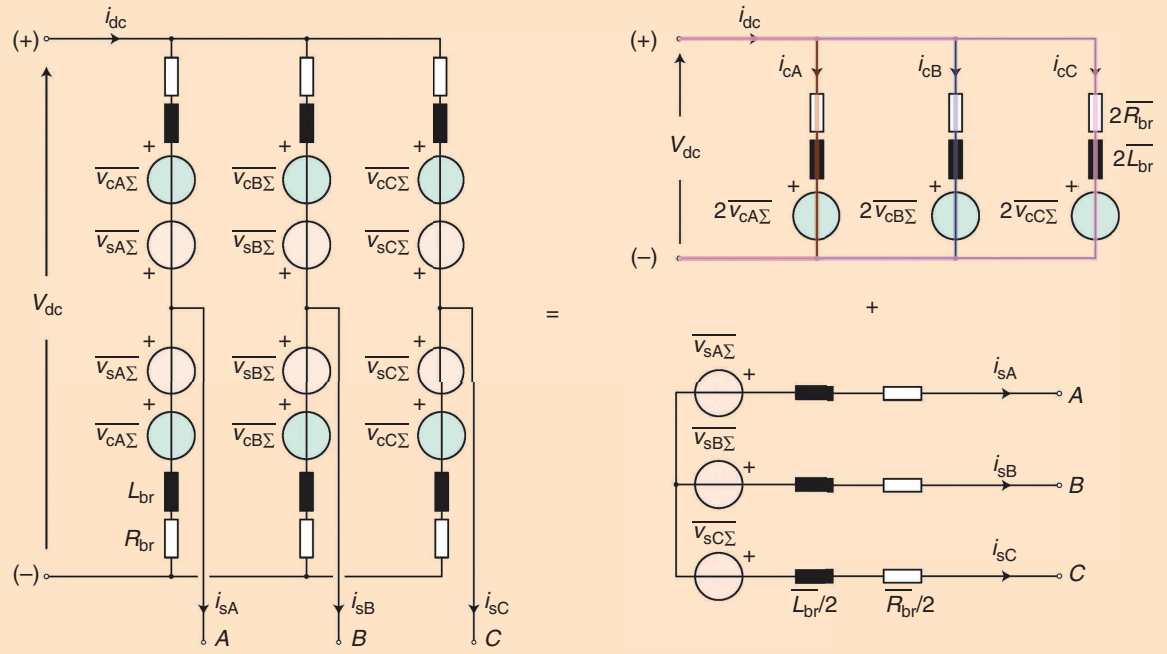

FIG 6 The simultaneous control of terminal currents requires every branch of the analyzed MMC to synthesize the voltage comprising two components, labeled with $\overline{v}_{c\{A/B/C\}\Sigma}$ (the dc component) and $\overline{v}_{s\{A/B/C\}\Sigma}$ (the ac component). As can be seen on the right side of the figure, two circuits, decoupled from each other, can be formed to identify the effect that each of the branch voltage components has on the control of terminal currents.

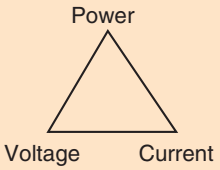

Current Sharing	Yes	No	No
Voltage Sharing	No	Yes	No
Power Sharing	No	No	Yes

FIG 7 Tradeoffs in the current, power, and voltage sharing of the parallel SBRs set. If a certain side of the triangle is chosen, equal sharing of the quantities positioned on the other two sides of the triangle cannot be achieved. For instance, equal current sharing requires the SBRs to generate different voltages, causing unequal power sharing. Similar reasoning can be applied to the other two cases.

However, equal energy distribution among the SBRs is considered the utmost priority of every MMC-based circuit. Therefore, in the structures containing parallel SBRs, the energy balancing must be given priority over the balancing of currents. Since every SBR produces the dc voltage that is approximately equal to the voltage of the dc grid the MMC is connected to (V_{dc}), the SBR power can be expressed as

$$P_{br,i} = P^*_{br} + \underbrace{\Delta P^{DC}_{br}}_{\frac{1}{2}V_{dc}\Delta I_{br,i}} + \underbrace{\Delta P^{AC}_{br}}_{\text{depends on } \Delta Z_{br}} . \quad (1)$$

Therefore, balancing of the SBR powers (energies) can be ensured through the intentional generation of the SBR

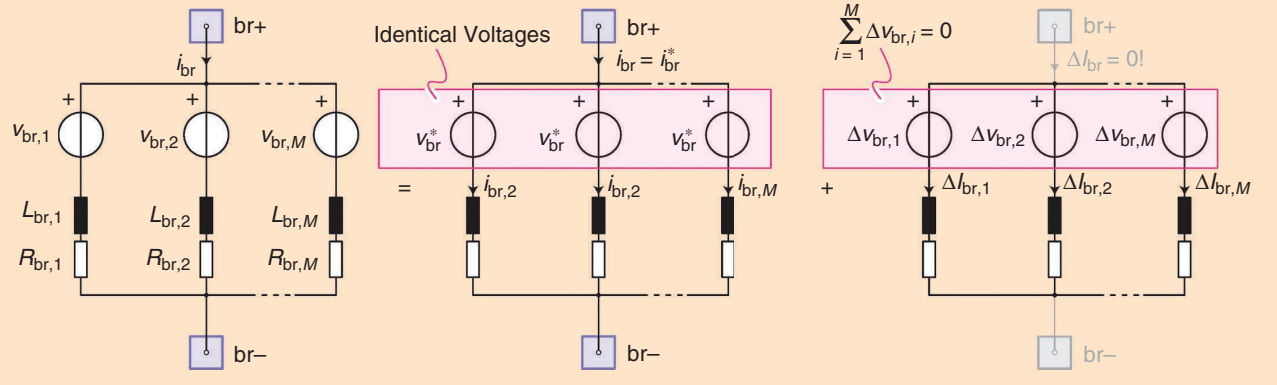

FIG 8 Balancing the SBR energies can be done through the intentional unbalances generated in the SBR dc currents. Namely, M voltage disturbances, the sum of which equals zero, result in M current components that sum to zero at the branch terminals (the right-most circuit). Consequently, the energy distribution among the SBRs can be affected.

dc current unbalances, labeled with $\Delta I_{\mathrm{br},i}$. Nonetheless, the unbalances $\Delta I_{\mathrm{br},i}$ must remain invisible from the terminals of an observed branch; otherwise, the control of the terminal currents gets corrupted. If $v_{\mathrm{br},i} = v^*_{\mathrm{br}} + \Delta v_{\mathrm{br},i}$ holds, the equivalent voltage seen from the terminals of an observed branch equals

$$\overline{v_{\mathrm{br}\Sigma}} = \frac{1}{M}\sum_{i=1}^{M} v_{\mathrm{br},i} = \underbrace{\frac{1}{M}\sum_{i=1}^{M} v^*_{\mathrm{br}}}_{v^*_{\mathrm{br}}} + \underbrace{\frac{1}{M}\sum_{i=1}^{M}\Delta v_{\mathrm{br},i}}_{\text{must be equal to zero}} . \tag{2}$$

As the equivalent circuit of a branch is linear, the superposition principle can be employed as depicted in Figure 8. According to (2), supported visually by Figure 5, if the sum of the SBR voltage disturbances $\sum_{i=1}^{M}\Delta v_{\mathrm{br},i}$ equals zero, the voltage seen between the branch terminals corresponds to the reference provided by the higher control layers. To put it differently, the SBR current/voltage unbalances, used for the internal branch energy balancing, do not affect the control of the MMC terminal currents since $\overline{v_{\mathrm{br}}} = v^*_{\mathrm{br}}$ (their effect cannot be observed from the branch terminals), as one can see from the right-most circuit in Figure 8.

To obtain the suitable set of the SBR dc current unbalances ($\Delta I_{\mathrm{br},i}$), the controller depicted in Figure 9 can be used. Namely, the mean energy of every SBR (from an analyzed branch) is calculated, based on the SMs voltage measurements, to set the individual SBR energy reference as the average of all of the measured SBR energies. Thereafter, the SBR energy deviations from the established reference are passed to the SBR energy-balancing controller, denoted by $H_{\Delta W}$. The output of this controller represents the SBR power component denoted by ΔP_{dc} in (1). Finally, the references $\Delta I^*_{\mathrm{br},i}$ are passed to the SBR current-balancing controller. Notice that, unless the controller part highlighted in green is included, this controller ensures the equal SBR current sharing, meaning that partial balancing of the SBR currents is always maintained, guaranteeing safe operation of the converter.

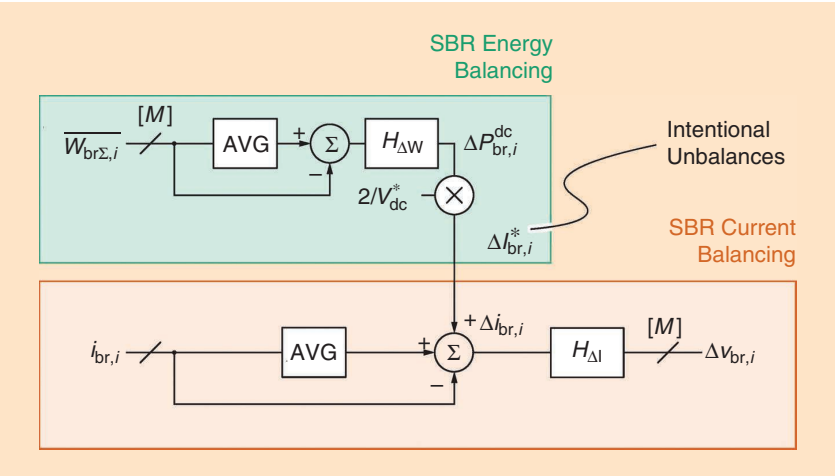

FIG 9 The SBR energy-balancing controller must be superimposed to the SBR current-balancing controller to ensure equal energy distribution among the SBRs. AVG: average.

It is noteworthy that the choice of the SBR current-balancing controller depends on the nature of the analyzed circuit. In the case the conventional 3PH-MMC is observed, the balancing of currents comprising dc and ac terms introduces the need for proportional (at least) along with the resonant controller parts. Considering that the SBR energy-balancing controller deals with the average energies, the conventional P (or PI) controller can be used to achieve satisfactory performance. Also, the use of other nonlinear control methods is possible, although this strongly depends on the control designer as well as the employed control platform.

Finally, the control block diagram of the structure depicted in Figure 4 can be presented as in Figure 10, from which one can

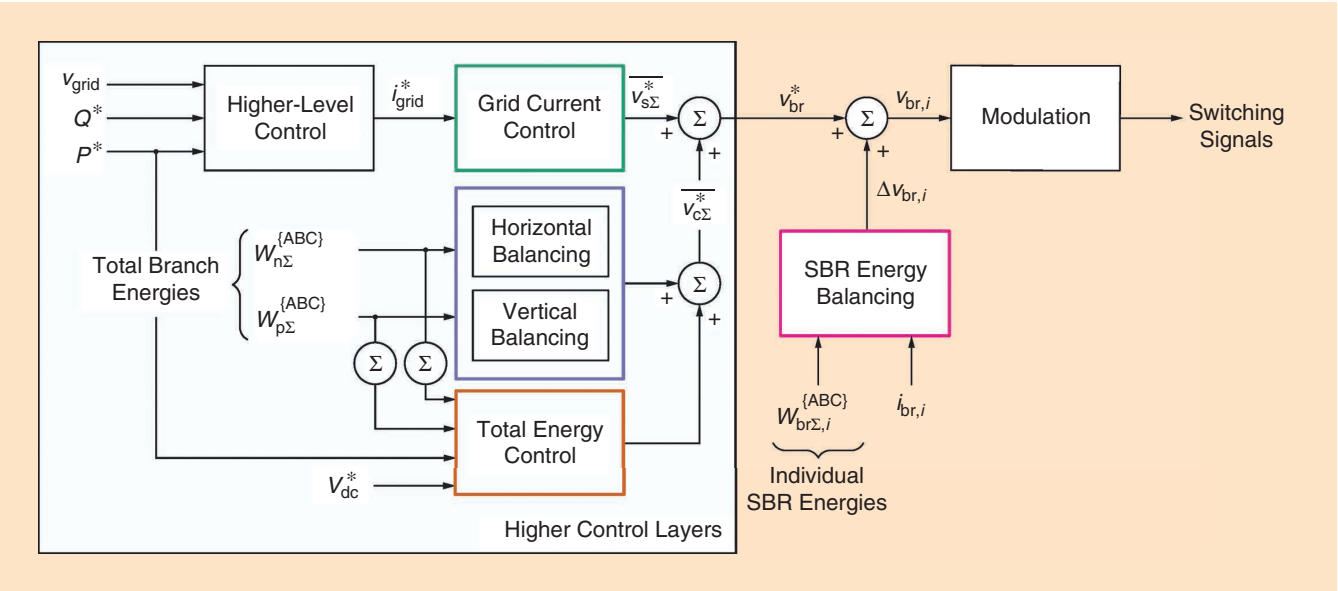

FIG 10 The control layers of the MMC operating with parallel SBRs.

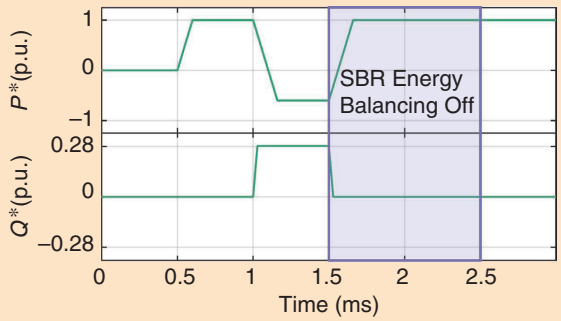

FIG 11 The reference power profile used to test the dynamic operation of simulated converters. In all of the simulated cases, the normalization was performed with respect to the rated powers provided in Table 1.

Table 1. The parameters of the simulated converters.

	Simulation 1	Simulation 2
Rated power (P^*)	1 MW	1.5 MW
Input voltage (V_{dc})	5 kV	5 kV
Number of SMs per SBR (N)	5	5
SM rated voltage (V_{SM})	1 kV	1 kV
SM capacitance (C_{SM})	0.83 mF	0.83 mF
Number of SBRs per branch (M)	2	3
SBR inductance (L_{br})	5 mH	7.5 mH
SBR resistance (R_{br})	60 mΩ	60 mΩ
PWM carrier frequency (f_c)	999 Hz	999 Hz

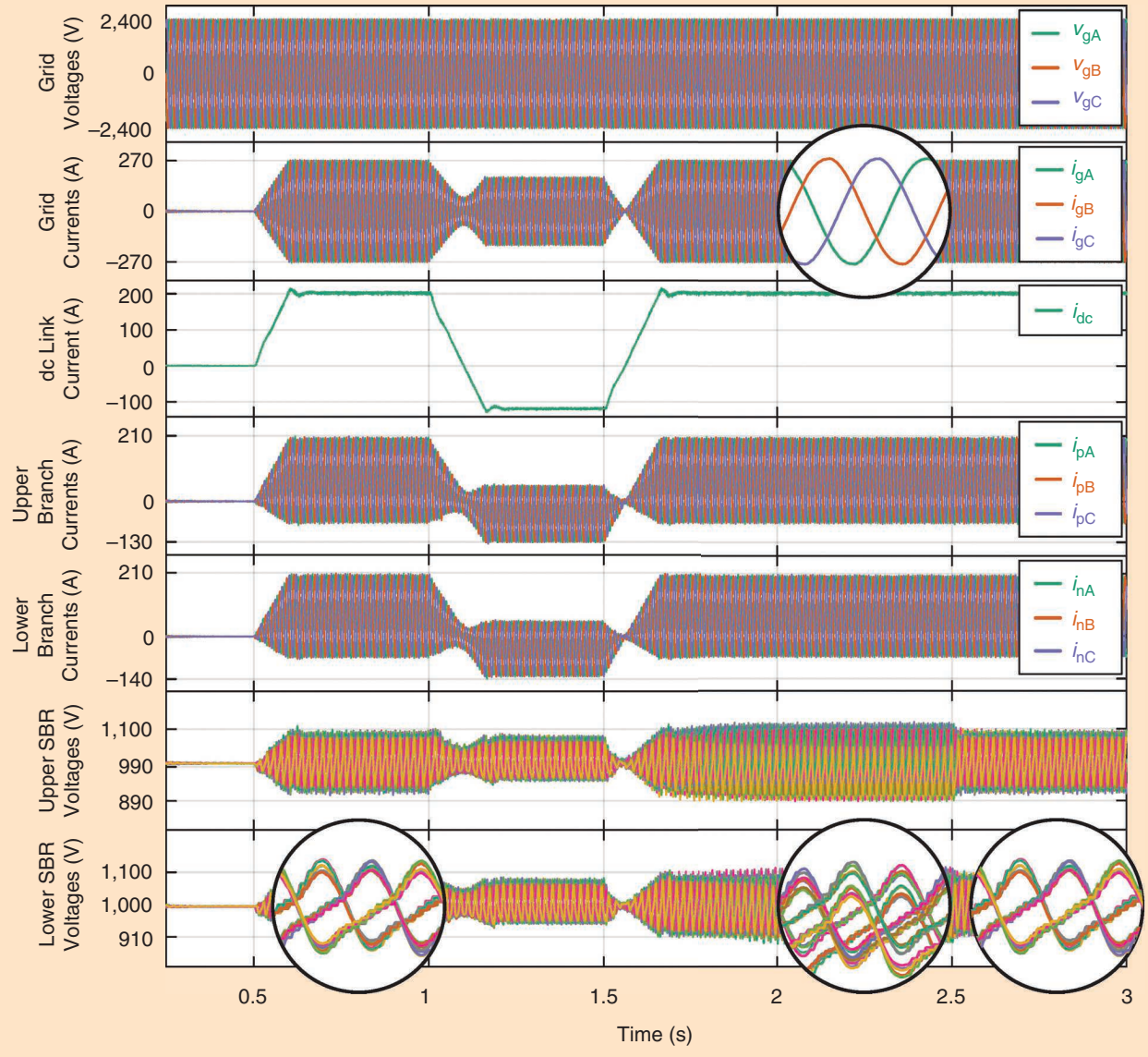

FIG 12 The operation of the converter utilizing two parallel SBRs within a branch.

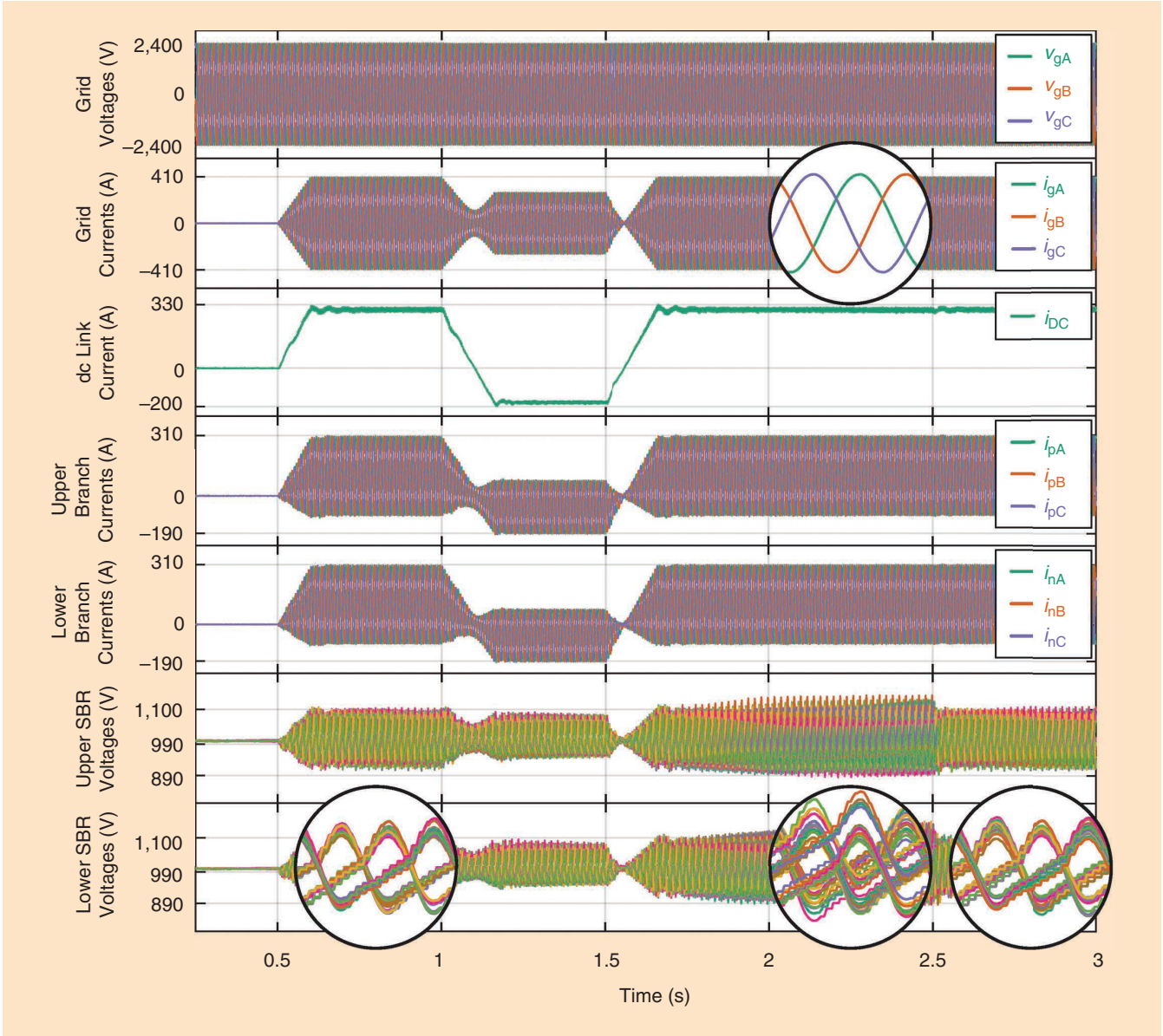

FIG 13 The operation of the converter utilizing three parallel SBRs within a branch.

notice that it is mainly occupied by the control blocks already known in the domain of the conventional MMC control. As indicated, another, although decoupled, control layer concerning the balancing of the SBR energies must be superimposed to the higher control layers. It is important to emphasize that the presented SBR energy-balancing method does not depend on the parity of the number of SBRs connected in parallel and this statement, which is verified shortly.

Simulation Results

The availability of an SM intended to serve the 0.5 MW converter, being connected to the 3-kV ac grid on one side and 5-kV dc grid on the other side is assumed. To demonstrate the possibilities of increasing the power capacity of the original converter, cases with two and three SBRs operating in parallel within a branch are simulated in PLECS. Consequently, the power rating of the original converter is doubled and tripled, respectively. Simulation parameters can be found in Table 1.

To test the dynamic performance of simulated converters, the reference power profiles defined in Figure 11 were followed. Furthermore, to demonstrate the importance of the SBR energy-balancing controller, its actions were disabled during the time interval $T_{W_{\mathrm{BAL}}}^{\mathrm{OFF}} \in [1.5\,s, 2.5\,s]$, as highlighted in Figure 11. To validate the proposed energy-balancing method while demonstrating its robustness, ±20% mismatches were randomly included in the SBR inductances as well as the SM capacitances.

Figure 12 presents the operation of the converter, utilizing two SBRs per branch, whereas Figure 13 illustrates the identical scenario, but with the converter utilizing three SBRs per branch. Both converters successfully track the reference power profile, which can be concluded based on the presented dc link current shape.

The lower-most plots present voltages of the lower SBRs, whereas zoomed-in parts tend to showcase the contributions of the additional SBR energy-balancing

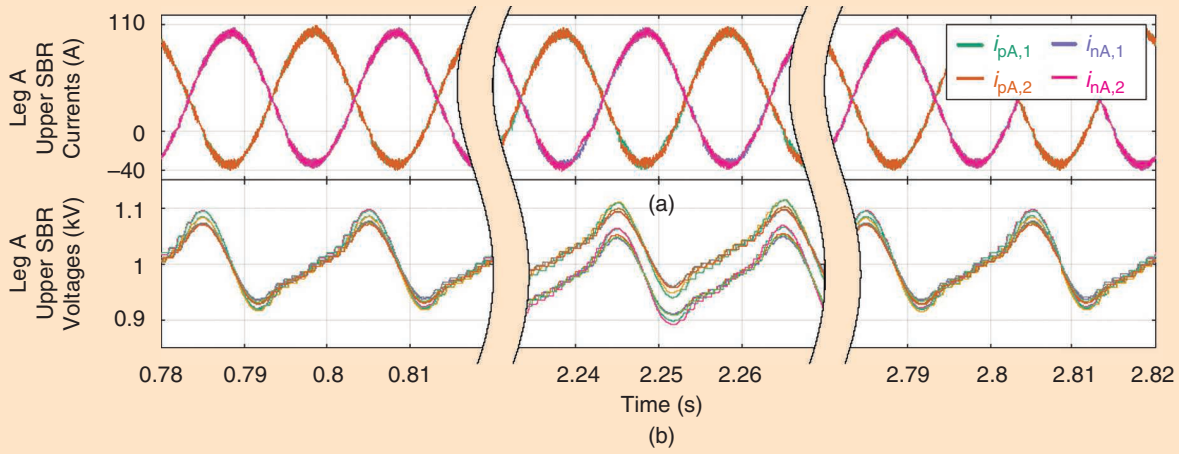

FIG 14 The (a) leg A upper and lower SBR currents and the (b) leg A upper branch voltages. In spite of the SBR currents being balanced, the SBR voltages tend to diverge in case the SBR energy-balancing controller is deactivated (middle part of the plot). The number of parallel SBRs per branch was set as $M = 2$.

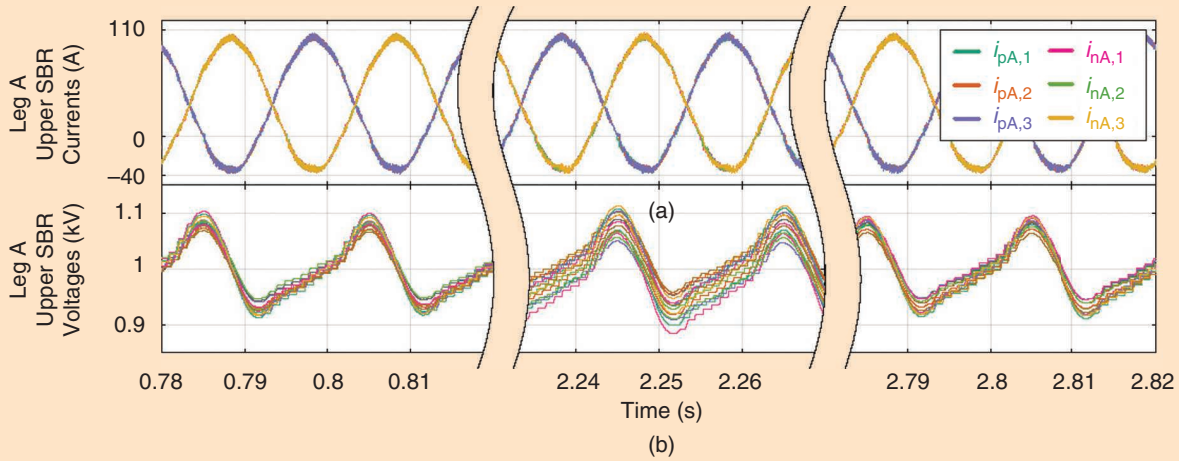

FIG 15 The (a) leg A upper and lower SBR currents and the (b) leg A upper branch voltages. In spite of the SBR currents being balanced, the SBR voltages tend to diverge in case the SBR energy-balancing controller is deactivated (middle part of the plot). The number of parallel SBRs per branch was set as $M = 3$.

controller. It can be observed that, before this controller was disabled, the SBR voltages remained perfectly balanced (the left-most zooms in on the bottom-most plots). However, upon its deactivation at $t = 1.5$ s, the SM voltages of all of the SBRs start to diverge (the middle zoomed-in images). At the time instant $t = 2.5$ s, the SBR energy-balancing controller was reactivated, resulting in the balanced SBR voltages in both of the presented cases (the right-most zoomed images).

Figure 14 presents the leg A lower and upper branch currents, along with the upper branch voltages, during the zoomed-in subintervals in Figure 12. SBR currents remain balanced, owing to the actions of the SBR currents-balancing controller presented in Figure 9. However, notwithstanding the SBR currents balance, SBR voltage divergence can be observed in the middle plot, which corresponds to the period at which the SBR energy-balancing controller was still deactivated.

Similar to Figure 14, the importance of the SBR energies-balancing controller, in case $M = 3$, can be observed from Figure 15. Conclusions identical to the ones already provided in the previous paragraph can be made.

Conclusions

This article presents the method of extending the power capacity of the MMC by paralleling its SBRs. The proposed control method enables the balancing of energies among the converter SBRs while keeping their currents partially balanced at all times. For an available SM design, the rated power of the converter can be effortlessly multiplied without the need for a major redesign of the existing converter parts. Consequently, the realization of cost-effective solutions that require minimal engineering efforts is enabled. Also, the proposed SBR energy-balancing method does not depend on the number of parallel SBRs. Hence, the scalability of the MMC depends exclusively on the

MMC Research Platform

Currently, the Power Electronics Laboratory, Ecole Polytechnique Fédérale de Lausanne, Switzerland, is finalizing its modular multilevel converter (MMC) platform, which will be used to support research activities like the ones presented in this article. The MMC submodule (SM) shown in Figure S1 is the full-bridge type and is based on the 1.2-kV insulated-gate bipolar transistors. The SM incorporates a flyback-based auxiliary power supply, DSP-based controller, protection logic, and circuitry involving fast temporary thyristor bypass and permanent relay bypass, as well as the fiber-optical communication link to the upper-layer controller. A complete cabinet system that will

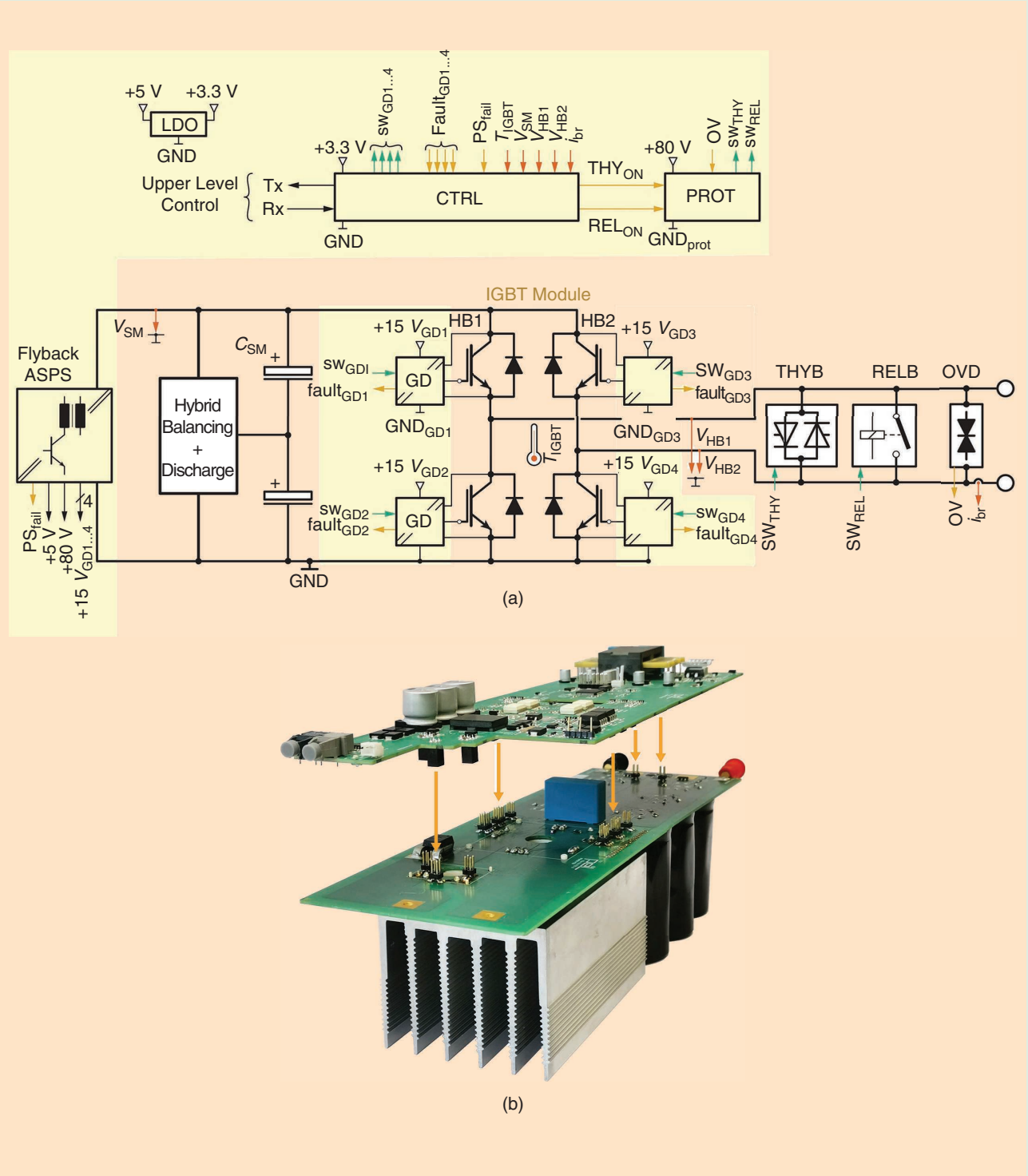

FIG S1 The MMC FB SM (a) principal layout and (b) implementation.

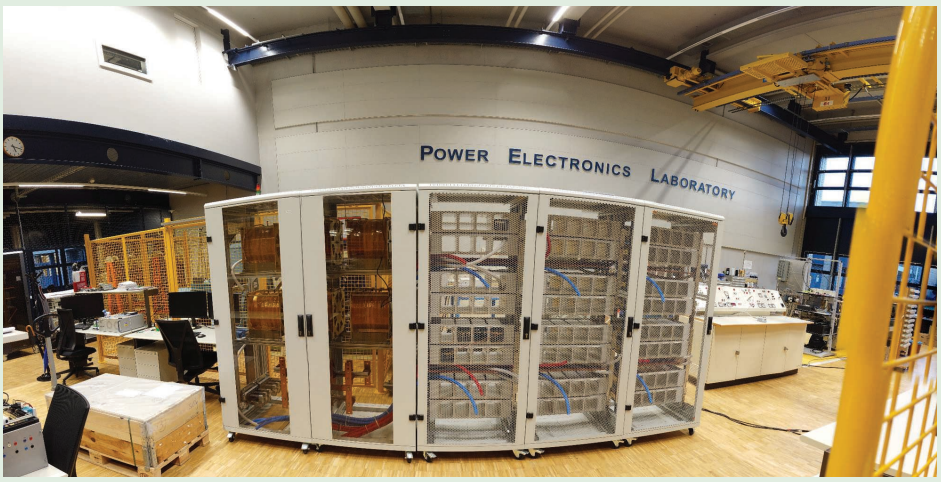

FIG S2 The MMC platform (in the assembly phase). The two left-hand side cabinets are hosting air-core branch inductances, while three cabinets on the right-hand side host SMs of two MMCs.

soon host two MMCs (a combined power of 0.5 MVA) is shown in Figure S2. Each MMC has 3.3-kV ratings on its ac terminals and ± 5-kV ratings on its dc terminals. A detailed description of the SM can be found in [S1].

Reference

[S1] M. Utvic, I. P. Lobos, and D. Dujic, "Low voltage modular multilevel converter submodule for medium voltage applications," in *Proc. PCIM Europe 2019; Int. Exhibition and Conf. Power Electronics, Intelligent Motion, Renewable Energy and Energy Management*, May 2019, pp. 1–8.

employed control platform, removing the SM hardware-design constraints from the list of possible factors limiting the amount of power reached with an existing SM design. The effectiveness of the proposed control method was validated under realistic conditions, implying the mismatches randomly distributed among the branch inductances as well as the SM capacitances. By means of the simple, well-known, and easily tuned linear controllers, the converter energy balance was ensured, indicating that extremely robust operation can be guaranteed. Upcoming research is discussed in "MMC Research Platform."

About the Authors

Stefan Milovanovic (stefan.milovanovic@epfl.ch) is a postdoctoral researcher with the Power Electronics Laboratory at the Ecole Polytechnique Fédérale de Lausanne (EPFL), Lausanne, Switzerland. He received his Dipl.Ing. and M.Sc. degrees from the University of Belgrade, Serbia, in 2015 and 2016, respectively, and his Ph.D. degree from EPFL in 2020, all in electrical engineering. His research is focused on medium- and high-voltage power conversion. He is a Member of the IEEE.

Drazen Dujic (drazen.dujic@epfl.ch) is an assistant professor and head of the Power Electronics Laboratory at the Ecole Polytechnique Fédérale de Lausanne (EPFL), Switzerland. He received his Dipl.Ing. and M.Sc. degrees from the University of Novi Sad, Serbia, in 2002 and 2005, respectively, and his Ph.D. degree from Liverpool John Moores University, United Kingdom, in 2008, all in electrical engineering. From 2009 to 2014, he was with ABB Switzerland, and since 2014, he has been with the EPFL. His research interests are predominantly related to high-power conversion technologies for medium-voltage applications. He has authored or coauthored more than 150 scientific publications and has filed 14 patents. In 2018, he received the EPE Outstanding Service Award, and in 2014, he received the Isao Takahashi Power Electronics Award for Outstanding Achievement in Power Electronics. He is a Senior Member of the IEEE.

References

[1] A. Lesnicar and R. Marquardt, "An innovative modular multilevel converter topology suitable for a wide power range," in *IEEE Bologna Power Tech Conf. Proc.*, 2003, vol. 3, pp. 272–277. doi: 10.1109/PTC.2003.1304403.

[2] A. Nami, J. Liang, F. Dijkhuizen, and G. D. Demetriades, "Modular multilevel converters for HVDC applications: Review on converter cells and functionalities," *IEEE Trans. Power Electron.*, vol. 30, no. 1, pp. 18–36, 2015. doi: 10.1109/TPEL.2014.2327641.

[3] J. Kolb, F. Kammerer, M. Gommeringer, and M. Braun, "Cascaded control system of the modular multilevel converter for feeding variable-speed drives," *IEEE Trans. Power Electron.*, vol. 30, no. 1, pp. 349–357, 2015. doi: 10.1109/TPEL.2014.2299894.

[4] A. Volke, J. Wendt, and M. Hornkamp, *IGBT Modules: Technologies, Driver and Application*. Neubiberg, Germany: Infineon, 2012.

[5] R. Hermann and S. Bernet, "Parallel connection of integrated gate commutated thyristors (IGCTs) and diodes," *IEEE Trans. Power Electron.*, vol. 24, no. 9, pp. 2159–2170, 2008. doi: 10.1109/TPEL.2009.2021837.

[6] M. Vasiladiotis, N. Cherix, and A. Rufer, "Accurate capacitor voltage ripple estimation and current control considerations for grid-connected modular multilevel converters," *IEEE Trans. Power Electron.*, vol. 29, no. 9, pp. 4568–4579, 2014. doi: 10.1109/TPEL.2013.2286293.

[7] M. M. Steurer et al., "Multifunctional megawatt-scale medium voltage DC test bed based on modular multilevel converter technology," *IEEE Trans. Transp. Electrific.*, vol. 2, no. 4, pp. 597–606, 2016. doi: 10.1109/TTE.2016.2582561.

[8] S. Milovanović and D. Dujić, "On facilitating the modular multilevel converter power scalability through branch paralleling," in *Proc. IEEE Energy Conversion Congr. and Expo.*, 2019, pp. 6875–6882. doi: 10.1109/ECCE.2019.8911850.

[9] A. Antonopoulos, L. Angquist, and H.-P. Nee, "On dynamics and voltage control of the modular multilevel converter," in *Proc. 13th European Conf. Power Electronics and Applications*, 2009, pp. 1–10.

PEM